[AMERICAN JOURNAL OF SCIENCE, VOL. 273, DECEMBER, 1973, P. 853-876]

American Journal of Science

DECEMBER 1973

MECHANISMS OF FLOW IN NATURALLY AND EXPERIMENTALLY DEFORMED PERIDOTITES

A. NICOLAS, F. BOUDIER, A. M. BOULLIER
Laboratoire de Géologie Structurale, Nantes, France

ABSTRACT. During experimental deformation of a synthetic dunite, a strong fabric developed by intracrystalline gliding in olivine. The first stage of the deformation process is rotation of anisometric crystals. After some 30 percent compressional strain, it is succeeded by gliding. With over 40 percent, syntectonic recrystallization at the highly strained boundaries of crystals becomes significant.

The developed structures and fabrics compare favorably with natural ones, supporting our previous interpretation and specifying the proposed method of kinematic analysis in Alpine-type peridotite massifs. The structures and fabrics characteristic of the inferred flow mechanism are found in many xenoliths, showing that it is operative in the areas of the mantle where basalts are generated. They also occur in harzburgites belonging to the ophiolite suite and regarded as representing the uppermost oceanic mantle. It is concluded that this flow mechanism is operative under the oceanic ridges and is responsible for the mantle anisotropy according to Francis's interpretation (1969).

INTRODUCTION

The success of the plate tectonics theory is renewing interest in the question of flow mechanisms in peridotites on the hypothesis that the plate motions may be attributed to flow in peridotites of the upper mantle. For example, the seismic anisotropy of the oceanic mantle is considered as being due to the fabric induced by flowage in peridotites (Hess, 1964). Avé Lallemant and Carter (1970), from experimental evidence, propose that the dominant mechanism of flow is syntectonic recrystallization. Nicolas and others (1971) and Nicolas, Bouchez, and Boudier (1972) have concluded from field evidence that translation gliding in olivine and enstatite is the main mechanism and that syntectonic recrystallization is secondary.

In this paper, we present new experimental evidence and more data from natural peridotites which specify the relative importance of the two mechanisms and the method of kinematic analysis of natural peridotites already described (Nicolas, Bouchez, and Boudier, 1972). The dynamic origin of the flow will also be investigated (simple shear versus pure shear). Our previous data on natural peridotites were only from Alpine-type massifs (Thayer, 1960); the fabric could have formed by the flow during crustal intrusion. A comprehensive study of the structures and fabrics of nodules from both continental and oceanic basalts (Mercier, 1972) leads to the conclusion that the massif-type structures and fabrics are widespread in the upper mantle and consequently that the same type of flow operates in the mantle.

EXPERIMENTAL DEFORMATION

Starting material.—The material selected was a synthetic dunite provided by C. B. Raleigh and produced from arc-melting of natural olivine. The reasons for this choice were that the rock is particularly dry. (H_2O^+ above 150° = 0.12 percent), devoid of any lattice fabric (fig. 1A), and fine grained (0.25 mm avg) (pl. 1-A) so that several hundred grains are present in the thin section cut in a core. Olivine (100 percent Fo)[1] is the only mineral. It contains small round-shaped bubbles (0.01 mm) which were used to calculate the amount of strain for each crystal (p. 860). It is believed that they do not significantly modify the mechanical properties of the dunite, because the modes measured on the samples selected for the experiments show that their volume is only 3 percent of the rock. The shape anisometry of the olivine crystals is large: [010] = 1; [001] = 1.8; [100] = 2.4 (pl. 1-A).

Apparatus—experimental conditions.—Five successful runs were performed in Raleigh's rock deformation laboratory at the National Center for Earthquake Research of the U.S. Geological Survey, on the large Griggs apparatus (Griggs, 1967) with cores of dunite 0.6 cm in diameter by 2 cm in length. They were carried out in compression at constant strain rate of around 10^{-5}/sec in the range of 13 to 15 kb and 1200° to 1300°C, usually with a high percentage of deformation in order to develop new fabrics. In many runs, after the completion of deformation, the samples were stress-annealed by stopping the movement of the piston for 10 hrs in the same PT conditions. The general description of the experiments conforms with that given by Carter and Avé Lallemant (1970) except for the following differences:

Our sample assembly had the following section: sample (O.D. 0.635 cm); inner sleeve (O.D. 0.875 cm) of alsimag, a dry, machinable ceramic; graphite furnace (O.D. 0.930 cm); alsimag sleeve (O.D. 1.780 cm); talc sleeve (O.D. 2.520 cm). S. H. Kirby designed it for us; the talc sleeves were changed for alsimag, in order to keep the sample as dry as possible at a high temperature. The alsimag sleeve, nearly as strong as the dunite itself, favors a continuous plastic deformation in the sample without fracturing. The thermal gradient in the specimen was reduced by using alumina end pieces above and under it, as illustrated by the regular longitudinal pattern of carbon diffusion from the furnace. In order to avoid lead diffusion through the sample, the lead washer was replaced by a copper washer, the only drawback being that about 10 percent of the total strain had to be applied until the nominal conditions of the run were reached, that is at the lower pressures and temperatures. The recording of the physical parameters of the runs (confining and load pressures, temperature, total strain percentage) is again consistent with Carter and Avé Lallemant's, with the same uncertainty regarding the

[1] This special composition together with the dryness of the rock may explain both its strength compared to natural dunites and the fact that a higher temperature is needed to complete a given state of deformation.

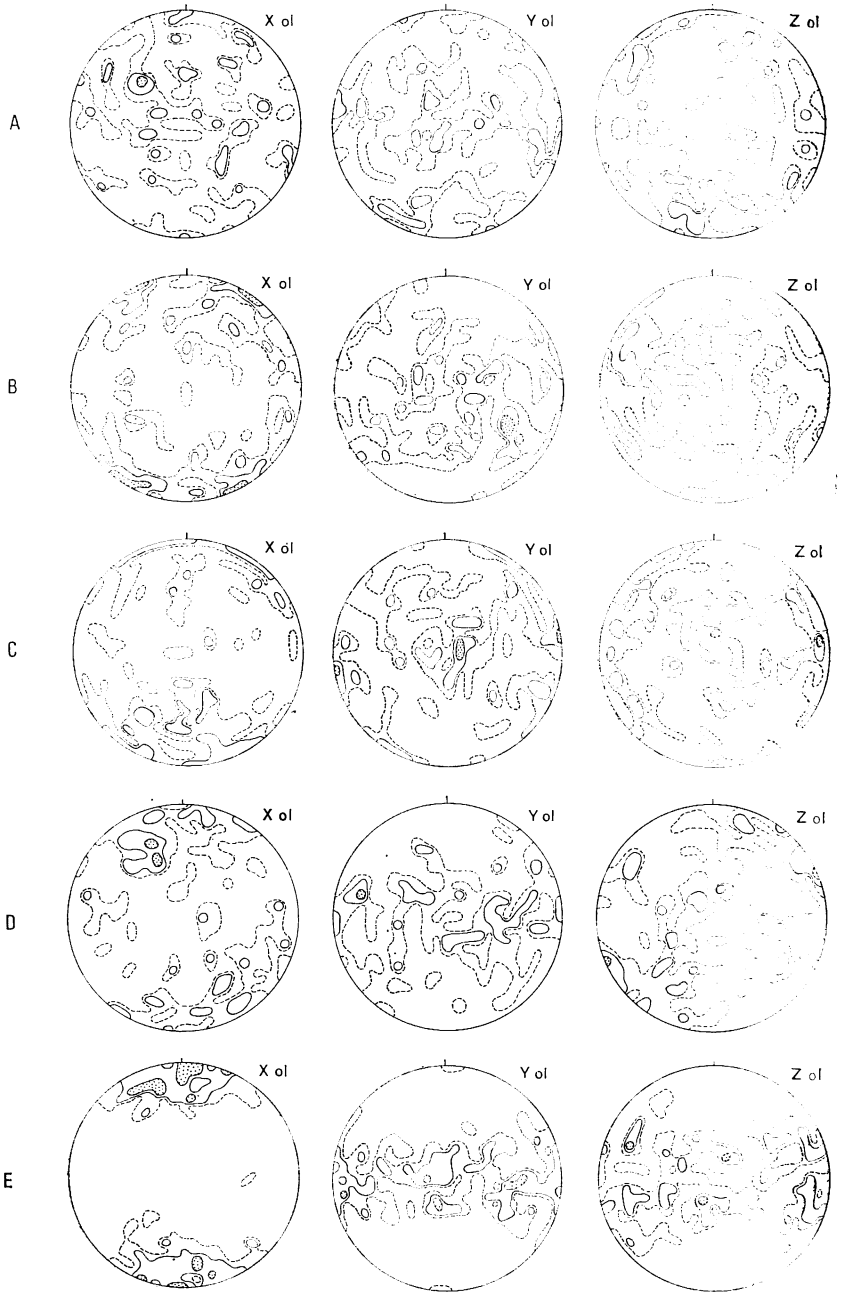

Fig. 1. Fabrics of large strained olivines in experimentally deformed dunite, represented by equal-area projections on the lower hemisphere. σ_1 is oriented vertical. Contours are at 1 percent (dashed line); 2 percent (continuous line); 4 and 8 percent (decorated areas); measurements on 100 grains.

A. Starting dunite, cored parallel to the following deformed samples (pl. 1-A)
B. 20 percent strain; T = 1250°; P = 13 kb; strain rate 10^{-5}/sec.
C. 33 percent strain; T = 1250°; P = 13 kb; strain rate 10^{-5}/sec (pl. 3-A).
D. 44 percent strain; T = 1300°; P = 14 kb; strain rate 10^{-4}/sec and 10^{-5}/sec (pls. 1-B and 2-A).
E. 58 percent strain; T = 1300°; P = 14 kb; strain rate 10^{-4} and 10^{-5}/sec. (pl. 1-B).

PLATE 1

A.

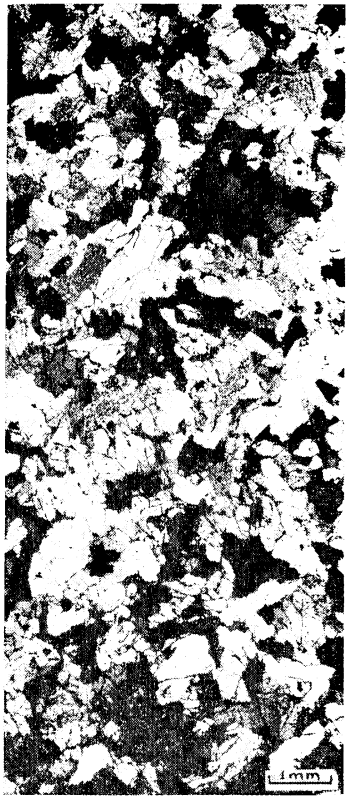

B.

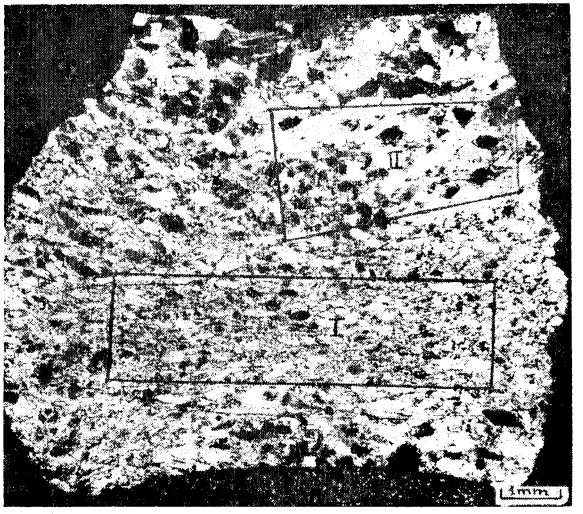

A. Synthetic dunite, starting material (crossed nicols).

B. 40 percent mean strain, σ_1 vertical (crossed nicols). The delineated domains have respectively 58 percent strain (domain I, fabric on fig. 1E) and 44 percent strain (domain II, fig. 1D and pl. 2-A).

pressures. The total axial strain determined from displacement of the piston gives a very poor idea of the actual strain on the specimen itself and is not representative of its distribution inside the specimen. Those values are critical here. They have been estimated by comparing the original diameter D1, with the present diameter D2. The percentage of axial strain is:

$$\varepsilon = 100 \left(1 - \frac{D1^2}{D2^2} \right) \text{ percent}$$

Results of the experiments.—The experiments with high strain lead to barrel-shaped specimens (pl. 1-B). The evolution of the fabrics with increasing strain is illustrated by figure 1. Except for the strain, the only significant variable in those experiments is the temperature, which ranges from 1200° to 1300°. By comparing equally strained samples, it can be concluded that the temperature differences within this range are not critical in the development of fabrics, but during the subsequent annealing the 100°C difference has a strong influence on recovery and postdeformational recrystallization.

From the study of structures and fabrics due to increasing strain the following two stages can be distinguished:

1. From 0 percent to about 30 percent strain: body rotation (figs. 1B, 1C). The minerals undergo first a bodily rotation which brings their shortest dimension [010] = X progressively closer to the maximum principal compressive σ_1; the minerals' shape is slightly altered. A limited amount of gliding is necessary for this rotation. The active directions are [100] = Z and [001] = Y[2]. For the crystals with those directions close to σ_1, rotation is helped by very intense kinking which also contributes significantly to the shortening. This deformational process is demonstrated by the study of the strain in bubbles (p. 860). The rotation results in a fabric in which Z and Y migrate toward the normal to σ_1, and X toward this σ_1 direction. This stage of deformation is completed when Z and Y, which are the glide and elongation directions, are in the 45° range from σ_1. Then the resolved shearing stress on the active systems [100] (010), [100] (okl), [001] (110) (Raleigh, 1968; Carter and Avé Lallemant, 1970) is maximum and induces the glide with accompanying rotation in the same sense and wavy kink banding (see below).

2. Over 30 percent strain: translation gliding and recrystallization (figs. 1D, 1E, 2A). With over 30 percent strain, the gliding mechanism is mainly responsible for the subsequent development of fabrics. This is

[2] Gliding along the [001] (110) system is demonstrated by the study of the kink banding (see also fig. 6B). It is not the dominant slip system above 1000° (Carter and Avé Lallemant, 1970), whereas in our experiments the nominal temperatures were in the 1200° to 1300° range. This discrepancy is due to the conditions of our runs in which 10 percent of the deformation is induced at temperatures lower than the nominal ones (p. 854); the [001] (110) gliding occurred then. This has been demonstrated by the total absence of this glide system in a specimen in which the strain was entirely induced at 1200°C (15 kb, 10^{-4}/sec). This sample was kindly provided by S. H. Kirby.

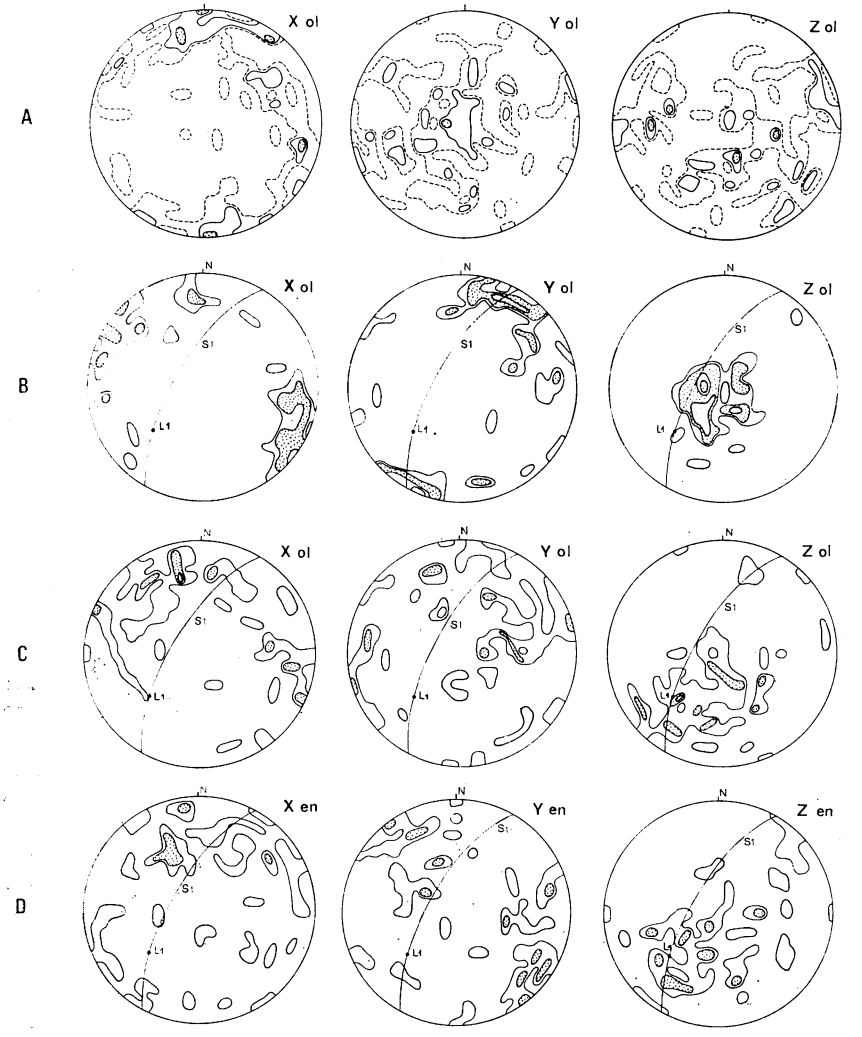

Fig. 2. A. Fabric of 100 small recrystallized olivine (as in pl. 2-A), same section as figure 1-E (annealing for 10 hrs at the nominal temperature).

B.C.D. Fabric of a naturally deformed lherzolite from Lanzo massif. Projection in horizontal plane; S_1 = foliation; L_1 = aggregate lineation regarded as an "a" kinematic direction. Contours as in figure 1; 50 grains.

B. Large and strained elongated olivines (ol). The obliquity of the fabric in relation to the foliation is regarded as a result of a dominant simple shear.

C. Small polygonal olivines (ol).

D. Large strained and dismembered enstatites (en).

demonstrated conclusively by the study of bubbles (p. 860) which points to a strong simple shear (fig. 3) inside the correctly oriented crystals. As a result, the shape of the grains is more and more elongated with wavy kink-banding normal to Z, thought to be due to differential movement and twisting of the lattice (Nicolas and others, 1971). The few crystals that still have their Z axis parallel to the stress direction are severely kinked with a high angle of rotation on both sides of the kink band boundaries. As demonstrated by the bubbles, those crystals are thus shortened along the compression direction. The elongation is responsible for the dismembering of grains and the observed grain size reduction (p. 865). The gliding produces a passive rotation of the crystals which progressively turns their Z and Y directions toward the plane normal to σ_1 and X parallel to σ_1. For large strains (figs. 1D, E), the Y direction shows a better concentration in the plane normal to σ_1 than the Z direction. With [100] (010) as dominant glide system (Z = glide line, Y = normal to Z in the glide plane), this is explained considering that the resolved shear stress in Z direction requires, for the gliding to be effective, that Z always remains at some angle to the plane normal to σ_1. On the other hand for a given orientation of Z, the resolved shear stress in the glide plane is maximum if Y lies in this plane.

As soon as the dominant gliding mechanism is initiated, a strong differential movement takes place in crystals as demonstrated by the intense and irregular elongation of bubbles. It seems to be more important in the regions of grain boundaries which are so intensely deformed that it may be impossible to delineate them. This can happen at the expense of crystals with a presumably unfavorable starting orientation in the strain field. The storage of strain energy in those domains readily induces syntectonic recrystallization, producing grains too minute to be measured under the microscope. If the strain rate is low enough (10^{-6}/sec as in some of Avé Lallemant and Carter's experiments) or if the sample is annealed, grain growth can be observed at the expense of the tiny grains first formed, and finally of the large strained ones, as described in quartz (Green, Griggs, and Christie 1970; Tullis, Christie,

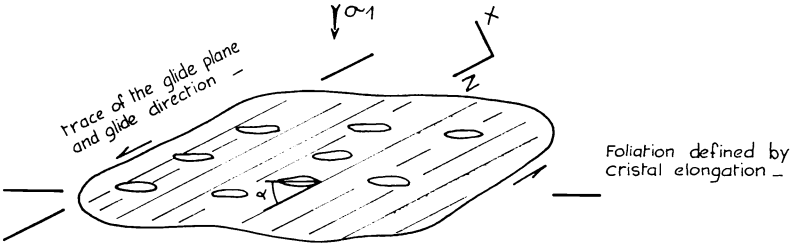

Fig. 3. Relative orientation of deformed bubbles to their host crystal and to the stress field (see also pl. 2-B). The angle α is correlated to the shear angle θ on figures 4 and 5.

and Griggs,[3] 1973). The latter authors have succeeded in producing plastic flow in quartzites experimentally. Their descriptions match ours in dunite remarkably. For a strain exceeding about 40 percent, the recrystallization becomes significant. In the most deformed sample with 58 percent strain (fig. 1E), after 10 hrs of stress-annealing at 1300°, the volume of recrystallized grains is almost equal to that of the large strained crystals. Figure 2A illustrates the fabrics of the recrystallized grains from that domain. Unfortunately, they were not big enough for their orientation to be measured except along one wall of the sample (pl. 2-A). The local heterogeneity in the stress and strain distribution might account for the secondary X maximum normal to σ_1 which does not exist in Avé Lallemant and Carter's recrystallization diagrams.

Deformation of the bubbles.—The bubbles inside the olivine crystals provide an excellent means of studying their internal deformation. Originally spherical, they are deformed with progressive strain to more and more flattened ellipsoïds (pl. 2-B). Figure 3 is a sketch of the relative orientation of deformed bubbles with their host crystal; it leads to the following conclusions.

The deformation geometry of individual bubbles compares very well with that of the whole crystal (fig. 3). This indicates that the mechanical process responsible for the deformation of bubbles is also valid for the crystal. The only significant difference is in the flattening ratio which is smaller in the crystal than in the bubbles; this is due to formation of new grains in highly strained crystals.

In a crystal devoid of twisting or kink banding, the bubbles tend to be of rather similar shape and orientation, suggesting that the internal deformation of the crystal is homogeneous. In the first stage of the deformational process when kinking and twisting are intense, the geometry of bubbles is more complex.

As shown in figure 3, the relation between the orientation of bubble elongation[4] and the glide direction Z or Y (known by studying the KBB) always indicates, according to our interpretation, a sense of simple shearing in agreement with the σ_1 orientation relative to the crystal.

The sections of crystals devoid of any indication of gliding (absence of kink banding) are usually the YZ plane or the YX plane; they are often round-shaped, and they display bubbles with a less elliptical sec-

[3] They conclude that some quartz "augen" which have remained relatively unstrained in a highly deformed matrix were initially oriented with their c axes parallel or perpendicular to σ_1 and thus were unsuited for basal slip. In our dunite, due to the strain markers in crystals represented by the bubbles (paragraph 2, this page), it has been possible to verify this interpretation. The olivine "augen" have been examined in highly deformed regions where they tend to have their slip planes normal to σ_1. Eighty percent of them showed evidence of an important slip probably accompanying a progressive external rotation toward their present position. Twenty percent had not slipped significantly, illustrating Tullis, Christie, and Griggs' interpretation.

[4] The elongation of the bubbles is estimated in a plane section (ZX, ZY, or YX). It cannot be disregarded that the principal axes of a bubble ellipsoïd could be oblique to these reference planes. The statistical ratios of elongation in the reference planes suggest that the longest axis of the bubbles ellipsoïd is in Z direction or close to it, and the shortest axis, parallel or close to X.

PLATE 2

A.

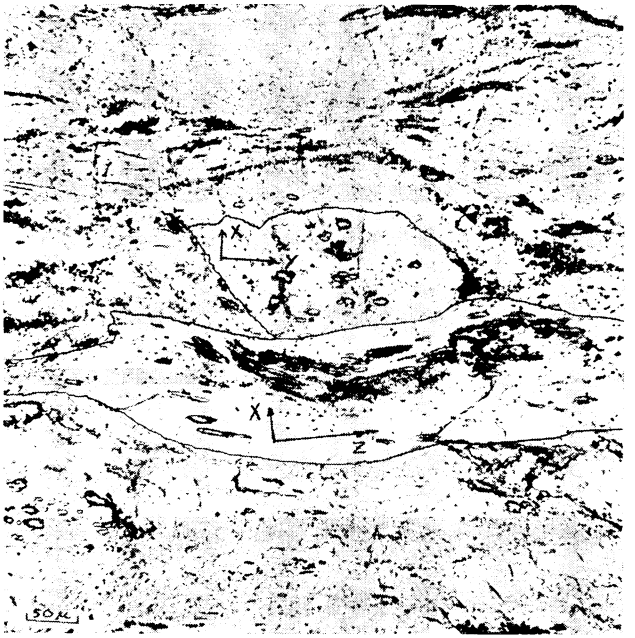

B.

A. Domain II of figure 1B, σ_1 vertical (crossed nicols). In the upper part of the picture simple shear is slightly dominant due to the lateral position of the domain in the specimen. Accordingly the large strained crystals are elongated mainly in one direction. Their boundaries recrystallize by annealing with a mosaic texture more clearly developed where the temperature was maximum as in the lower right angle (fabric in fig. 2A). In the center of the upper part of the picture, tight "compression" kink bands (KBB normal to σ_1) can be observed in contrast with wavy "torsion" kink bands (KBB parallel to σ_1) visible below to the left (see also pl. 3-A, -B).

B. Deformed bubbles in a ZX section with a geometrical pattern conformable with theoretical sketches of figures 3 and 4. On the other hand in the neighboring YX section, which does not contain any active glide direction, the sections of bubbles are less elliptic.

tion (pl. 2-B). All this strongly suggests a mechanism of deformation by translation gliding on to the systems evidenced by the wavy kink bands. It is due to the shear stress resolved on crystals oblique to σ_1.

The theoretical relationship between the flattening ratio of bubbles, the shear angle θ, and the angle of the long axis of their ellipse with the glide direction (angle α) is illustrated by figure 4; figure 5 illustrates the theoretical relationship between the angle α and the shear angle θ (demonstrated in the app). Considering the [100] (010) glide system to be the most active, our interpretation is reinforced by plotting in the favorable ZX plane, for all the studied samples, the ratio r of flattening of bubbles versus their angle α, as defined in figure 4 (fig. 6A). The point distribution is averaged by the theoretical curve r/α for ellipses submitted to increasing simple shear, showing incidentally that [100] (010) is the main glide system, as expected from the results of Carter and Avé Lallemant (1970).

Discrepancies from this curve may have three explanations:

1. For weak elongations of bubbles, the r ratio and the α angle are estimated very inaccurately.

2. Occasionally the glide system may be [100] (001) or [100] (okl) (pencil gliding of Raleigh, 1968). The glide plane being then parallel or oblique to the considered ZX plane, the angle α is lowered for a given shearing ($\alpha = 0°$ for [100] (001); α with intermediate values between 0° and those on the theoretical curve for [100] (okl).

3. Some crystals, with a special symbol in figure 6, have begun their deformation with the glide direction Z parallel or close to σ_1. During the first stage of deformation (rotation), they have suffered intense kink banding (KBB normal to σ_1) with high rotation of one band relative to the other, resulting in a shortening of about 20 percent as demonstrated by the ratio of flattening of the bubbles (pl. 2-A). The kink bands are so tight that one bubble usually overlaps several bands; its flattening may be a mean effect of slip in opposite directions from one band to the other. This is confirmed by the observation, in especially large bands, of individual bubbles

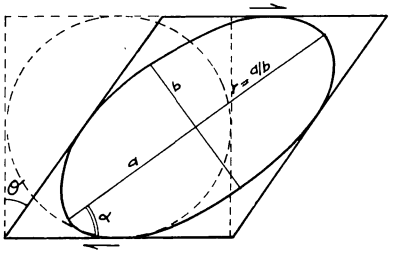

Fig. 4. Theoretical sketch of simple shear of a circular section of a bubble for a shear angle $\theta = 35°$. Flattening ratio a/b = 2. The angle α as defined on figure 3 is 54° for this particular value of θ (see fig. 5).

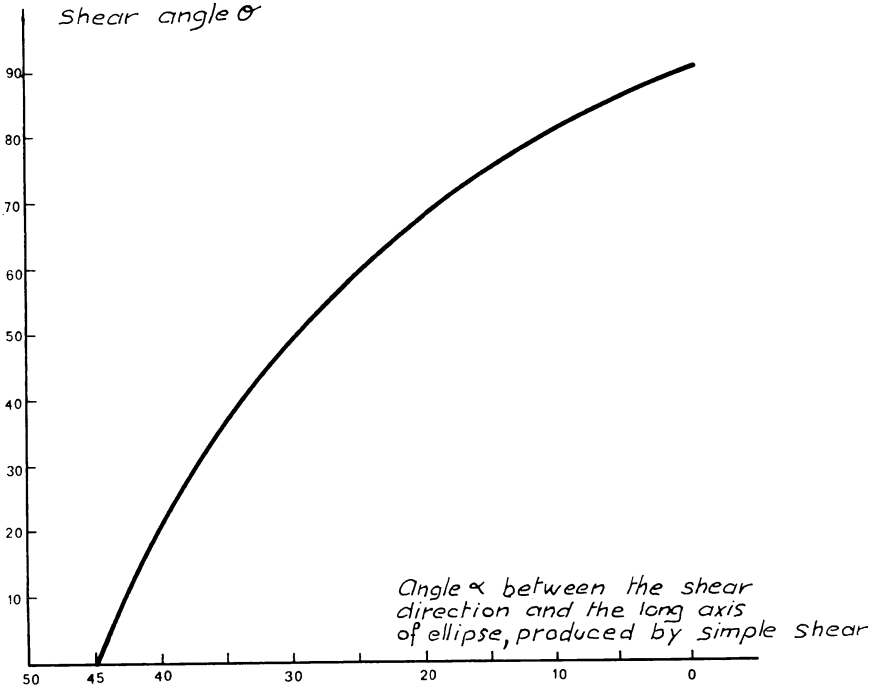

Fig. 5. Graphical relationship between the shear angle θ and the angle α as defined on figures 3 and 4 (calculations in app).

elongated in opposite directions from one band to the other. On figure 6A, their representative points contribute, for moderate to high values of α, to the observed clustering of the points above the theoretical curve.

Figure 6B represents the bubble deformation in the YX plane with the same coordinates. The trend of the points distribution in figure 6B supports the conclusion, evidenced by the kink banding, that the system [001] (110) is also active (see footnote, p. 860). The conclusions presented above for grains with their glide direction (now Y) close to σ_1 are still valid.

No comparable trends have been evidenced in the ZY plane, demonstrating the relative inactivity of the [100] (001) glide system.

Modification of grain shape.—With increasing strain, the grain size is reduced, and the shape is altered (figs. 7A and B). Though some uncertainty remains, due to difficulties in obtaining enough reliable measurements on the large strained olivine crystals considered here, the data in figures 7A and B can be interpreted as follows.

The first stage of the deformation ranging from 0 to 30 or 35 percent strain is characterized by a weak reduction of grain size (fig. 7A) and a moderate increase in shape anisometry (ratio statistically estimated in directions normal and parallel to σ_1) which could proceed in two

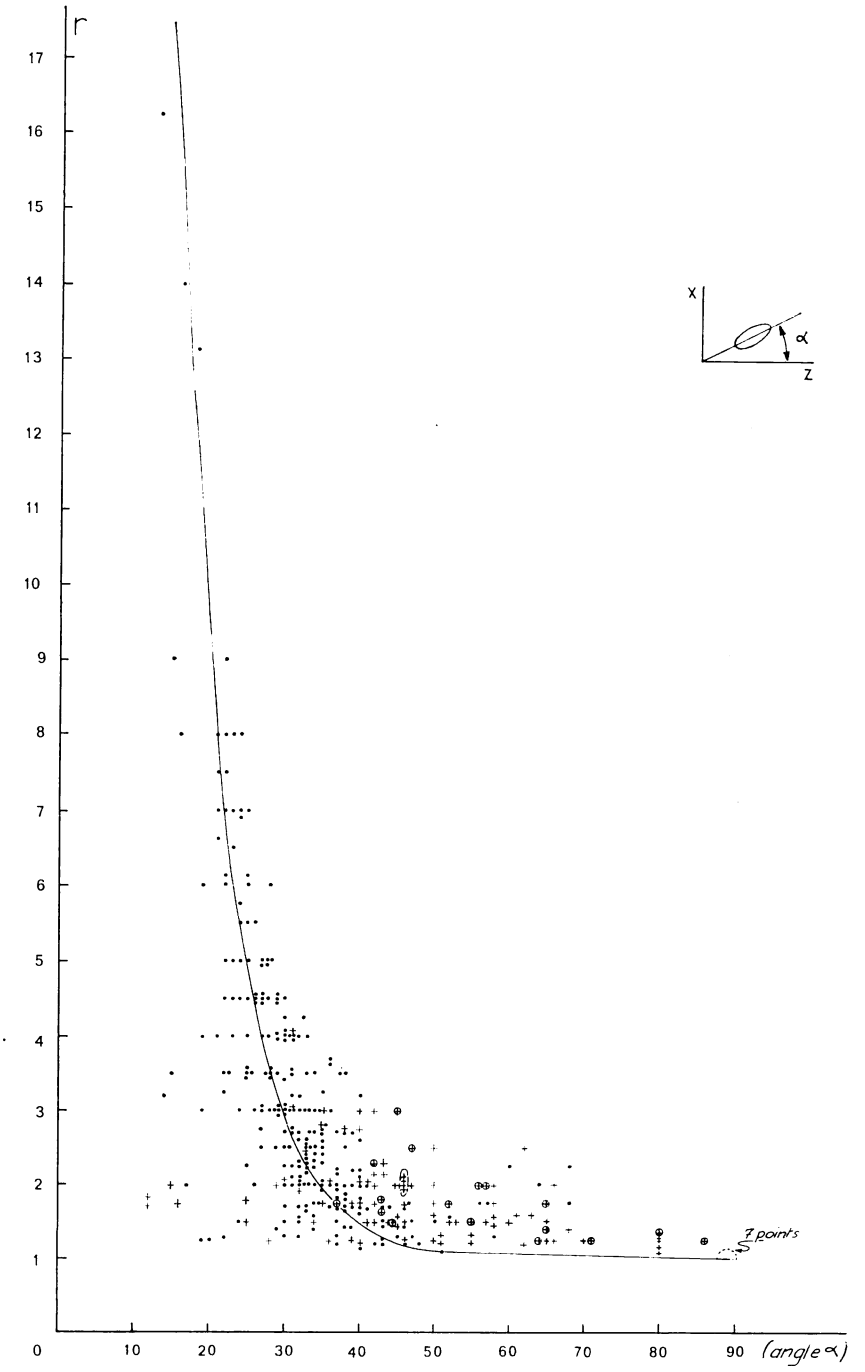
r
17
16
15
14
13
12
11
10
9
8
7
6
5
4
3
2
1
0
10
20
30
40
50
60
70
80
90
(angle α)
X
α
Z
7 points

6A.

steps: between zero and 10 percent strain, swift anisometry increase, and between 10 and 35 percent, a rather constant behavior. This first stage might correspond to the rotational process acting upon initially anisometric olivine grains (p. 857). It is not understood why the anisometry ratio should not increase progressively during this first stage. In fact the crude estimations presented here do not allow the ruling out of this possibility. The passive rotation of the grains would be a process inducing less internal strain than the subsequent gliding, and consequently the grain size could be affected only slightly.

In the second stage with over 30 to 35 percent strain, the grain size decreases while the shape anisometry ratio increases. This stage would correspond to intracrystalline gliding of the olivine grains now properly oriented in the stress field (p. 860). In this process the severely strained grains would tend to be dismembered and recrystallize. The grain size would rapidly decrease, and the shape anisometry ratio increase. The mean ratio of length in Z direction/length in X direction for individual grains changes from Z/X = 2.40 in the original dunite to Z/X = 2.74 in the dunite with 58 percent strain. In the latter, again only the large strained crystals are considered; their dismembering during gliding explains the smaller increase than expected in this ratio.

RELATION TO NATURAL DEFORMATIONS

When comparing the experimentally deformed dunite with Alpine-type peridotites plastically deformed at high temperature, one must bear in mind that in the experiments the stress field has an axial symmetry versus an orthorhombic one in natural rocks. Moreover the strain rate and time allowed for syntectonic and post-tectonic recrystallization are

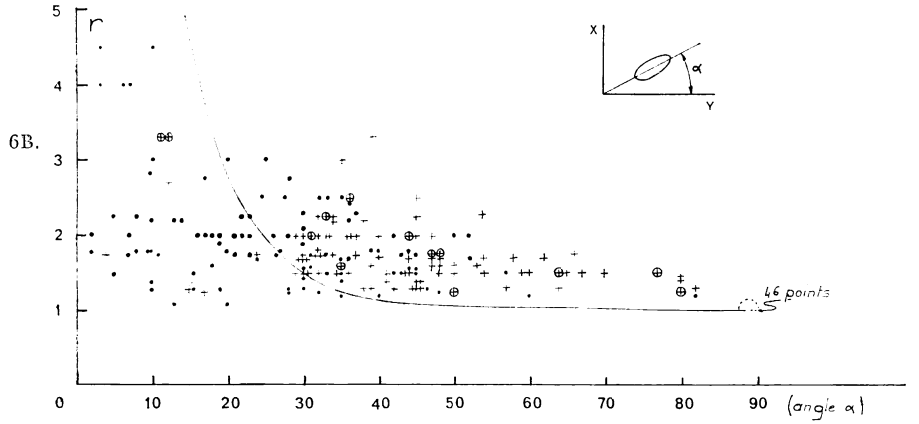

Fig. 6. Relationship between the elongation ratio "r" of bubbles and the angle α between this elongation and the glide direction. The traced line represents the theoretical relationship. Dots: bubbles in specimens with over 33 percent strain; crosses: under 33 percent strain; open circles: when the glide directions are still close to σ_1, which occurs only in specimens under 33 percent strain. A. Measurements in ZX plane; B. Measurements in YX plane.

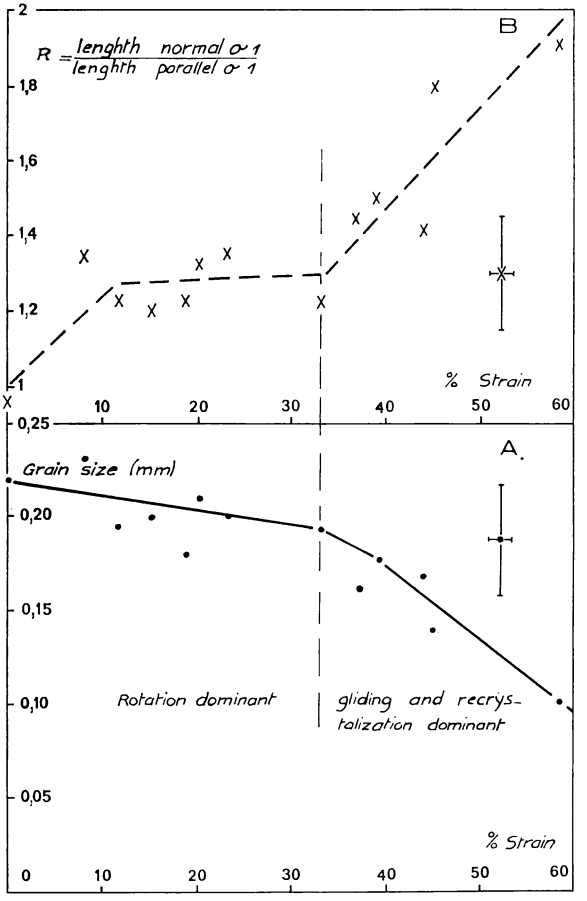

Fig. 7. A. Relationship between percent strain and grain size for the large strain crystals.

B. Relationship between percent strain and the ratio R of statistical elongation in the direction normal to σ_1 versus elongation parallel to σ_1 for large strained crystals.

respectively much quicker and shorter than in nature; as a result, for comparable structures in the experimentally deformed rock, the grain size is smaller by a factor of about 5.

Pure shear versus simple shear.—Another major difference between the structures and fabrics induced in the experiments and natural ones is that in natural peridotites we regard the foliation plane as generated not always by flattening but often by shearing because shear folds can be observed in the field, and, in many peridotites, the lattice fabric is slightly oblique, in a single direction, to the foliation plane defined by the elongation of crystals. This fabric (figs. 2B, C, D) can be readily overlooked and might be more common than first thought. It has been interpreted (Nicolas, Bouchez, and Boudier, 1972), in agreement with the present experimental conclusions on olivine crystals, as the result

of simple shear inducing gliding principally in one direction in the olivine and enstatite crystals. Therefore, we consider that in many Alpine-type peridotites and xenoliths the flow is induced by a simple shear, with a minor pure shear component, commonly acting parallel to older structures (layering). In some Alpine massifs like Baldissero (Italian Alps), the remarkable symmetry of the fabric, relative to the foliation, indicates a flow driven by pure shear (Nicolas and others, 1971, figs. 5D, 7). The experiments should be compared preferably to those natural occurrences. However, as already observed in experiments by Tullis, Christie, and Griggs (1973), some marginal areas of the deformed samples approximate simple shear regime (pls. 1-B and 2-A), whereas in the center of the sample it is axial compression. The textures in the two areas are identical except, in our runs, for a tendency for the lattice orientations to be oblique to the local foliation. This allows some comparison between experimental textures produced by pure shear and natural ones even though they have originated by simple shear.

Structures.—Despite these differences, the structures compare remarkably well (pl. 3-A and B). Both kinds of crystals visible in the experimentally deformed dunite, (A) the large elongated and strained grains with KBB at a high angle to the plane of flattening and (B) the small recrystallized ones, are found in the natural peridotites considered here. In both cases, the elongated crystals and the aggregates of small grains define a plane (flattening in experimentally deformed dunite, foliation in natural peridotites (Nicolas and others, 1971)). The analogy is better when the dunite cores are annealed, causing growth of the small grains and development of a mosaic structure at the boundaries of the large strained grains (compare pl. 2-A here with fig. 2 and pl. 1-B in Nicolas and others, 1971). Natural lherzolites considered as deformed by pure shear again display a structure very similar to some experimentally deformed samples (compare pls. 1-B and 2-A here with fig. 7 in Nicolas and others, 1971).

Fabrics.—The comparison of the fabrics of large strained olivine crystals is not so rewarding because of the difference in the stress fields (axial versus orthorhombic symmetry). In both cases a good [010] = X maximum tends to develop normal to the flattening and foliation plane[5] (figs. 1E and 2B). In experimentally deformed samples, [100] = Z and [001] = Y lie in the flattening plane normal to σ_1, without any preferred orientation. In this regard the fabric of the large strained crystals cannot be distinguished from that of the small recrystallized grains (Avé Lallemant and Carter, 1970).

[5] This tendency for X in the deformed samples (fig. 1E) can be explained in the interpretation of fabrics induced by gliding if it is considered that the dominant glide system is [100] (010) (p. 862). In natural peridotites (fig. 2B), X behaves in a similar way, though when the deformation is intense and presumably at lower temperature, it tends to form a girdle normal to the foliation plane and to a strong Z maximum lying in this plane or close to it. This compares favorably with the glide systems operative in either case (Nicolas and others, 1971; Nicolas, Bouchez, and Boudier, 1972).

PLATE 3

A.

B.

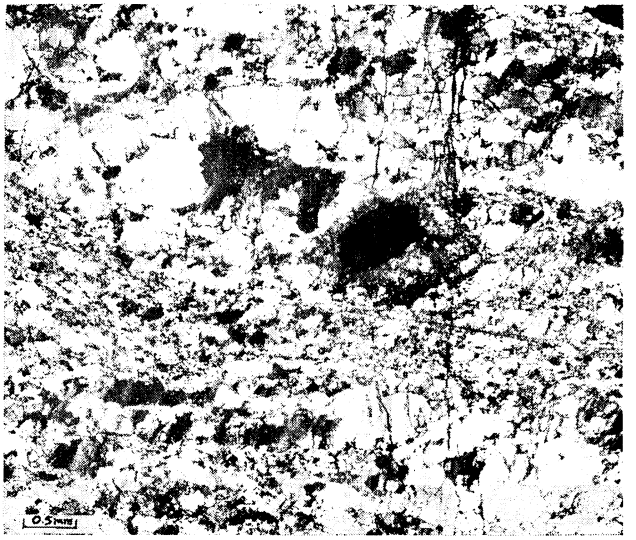

A. Specimen with 33 percent strain (fig. 1C) showing some very elongated olivine crystals, tending to be dismembered, surrounded by fragments of strained crystals in a finely recrystallized matrix.

B. Locana lherzolite with, as in (A), ribbon shaped olivine crystals surrounded by recrystallized grains. In this section the elongated olivines have a lattice fabric systematically oblique to the foliation as evidenced by the KBB. It would lead to a fabric similar to figure 2B interpreted as due to simple shear.

Mechanisms of flow.—The successive stages in the flow mechanisms of the experimentally deformed dunite can be correlated with the assumed mechanisms in naturally deformed peridotites. Starting with a random assemblage, the rotation of grains, accompanied by a moderate intracrystalline gliding which is observed in the deformed dunite, results in a fabric favorable to subsequent intense gliding. In natural peridotites no evidence of this stage has been reported. In fact, it would operate only if the grains in the initial assemblage had a strong shape anisometry and if the rock fabric was weak or misoriented relative to the new stress field. New results on the study of xenoliths (Mercier, 1972) and on the superimposed deformations in peridotite massifs (Nicolas and others, 1971; Nicolas, Bouchez, and Boudier, 1972) suggest that the peridotites submitted to a plastic deformation already had a weak lattice and shape fabrics and that in many instances the new shear plane is parallel or close to the older structures (compositional layering). Consequently X was already at a high angle to the foliation.[6] This stage of the deformation process would thus be avoided.

The intracrystalline gliding evidenced in the experimentally deformed dunite has been claimed by Nicolas and others (1971) as the dominant mode of flow in natural peridotites with minor syntectonic and post-tectonic (annealing) recrystallizations in contrast with Avé Lallemant and Carter (1970) who favor syntectonic recrystallization. Our interpretation was based on the textures and fabrics of olivine and enstatite, overlooking diopside because:

1. It usually represents less than 10 percent in peridotites.
2. The limited data (7) in literature on diopside fabrics *in peridotites* (Yoshino, 1964; Avé Lallemant, 1967; Möckel, 1969; unpublished data on Lanzo massif) indicate weak and insignificant orientations (3 cases) or contradictory ones (4 cases).

It is known experimentally that diopside is stronger than enstatite and olivine. Therefore it is suggested that in a flowing matrix formed by those two minerals, diopside could be inactive and passively rotated, resulting in the absence of preferred orientation and in a rather rounded shape which is often observed. In two cases out of seven (Yoshino, 1964) the preferred orientation of diopside is [010] = Y diopside parallel to [010] = X olivine, which in turn is considered by Avé Lallemant and Carter (1970) as parallel to σ_1. This is compatible with an origin by syntectonic recrystallization characterized by [010] = Y diopside parallel to σ_1 (Carter, Baker, and George, 1972). In the other two cases where the diopside has a distinct fabric this is definitely not true (Möckel, 1969).

[6] In our 1971 paper, we considered that the fabrics in rocks with a moderate plastic deformation (Nicolas and others, 1971, figs. 5A and B) were due to this deformation. We now think that they reflect an older fabric progressively modified by the plastic deformation. The new fabric completely obliterates the older one in more deformed rocks (Nicolas and others, 1971, figs. 5C and D). Accordingly the X maximum normal to the foliation is changed to a girdle, and the Z maximum greatly increases in intensity.

New experimental data on the development of preferred orientation in enstatite by syntectonic recrystallization (Carter, Baker, and George, 1972) give an opportunity to discuss the influence of this process on the enstatite fabric in peridotites. These authors describe [010] = X enstatite parallel to σ_1, that is normal to the foliation plane. We consider that the foliation plane is not necessarily normal to σ_1 (p. 866), but, since the fabrics are always closely related to this plane, available literature has been consulted for each case where the enstatite fabric and the foliation were presented together. Fifty two descriptions have been found for Alpine-type massifs and xenoliths from basalts and kimberlites: Collée, 1963 (2)[7]; Avé Lallemant, 1967 (6); Möckel, 1969 (10); Nicolas and others, 1971, Nicolas Bouchez, and Boudier, 1972, this paper (4); Etienne, 1971 (1); Mercier, 1972 (13); Boullier, and Nicolas, in press (1); Juteau written commun. (2); unpublished data on the following massifs: Lanzo, Italy (4); Ronda, Spain (2); Beni Bouchera, Morocco (2); Finero, Italy (1); Seiad, Calif. (1). Another estimation has been carried out taking the [010] = X olivine maximum as usually normal to the foliation and parallel to σ_1 in pure shear experiments. The enstatite axis which coincides with the X olivine maximum is then looked for. Sixty three descriptions are now available with the following new contributions: Collée, 1963 (3); Avé Lallemant, 1967 (1); Raleigh, 1965 (1); Brothers and Rodgers, 1969 (2); Kumazawa, Helmstaedt, and Masaki (1). The results are summarized in table 1.

TABLE 1
Review in literature of Y and X enstatite fabrics in peridotites with their relation to the foliation plane or the X olivine maximum

	Maximum of [100] = Y enstatite	Maximum [010] = X enstatite	No distinct maximum	Total number of data on enstatite fabric
Normal to the foliation plane	31	5	16 no distinct maximum and other relations	52
Parallel to [010] = X olivine maximum	25	5	33	63

From table 1 it can be concluded that for the peridotites investigated, the enstatite fabric is, in a large number of cases, compatible with an origin by translation gliding ([100] = Y maximum normal or at a high angle to the foliation or parallel to the [010] = X olivine maximum). It is more rarely compatible with an origin by syntectonic recrystallization ([010] = X normal to the foliation or parallel to X olivine).

However, our experiments show that for intense strain (over 40 percent) syntectonic recrystallization becomes significant together with

[7] Number of descriptions.

gliding (p. 859). Avé Lallemant and Carter (1970) experimentally developed fabrics by syntectonic recrystallization for weak to moderate strains but in a wet medium and often with a powder as a starting material; these conditions might explain the discrepancies in the results. Their results did not change when they performed some runs with a natural dunite in a dry medium but at a slower strain rate than ours (10^{-6}/sec instead of 10^{-5}/sec). The slower strain rates and possibly a higher temperature may have favored recrystallization over gliding as is observed in quartzites by Tullis, Christie, and Griggs (1973). Avé Lallemant and Carter's recrystallized textures do not show obvious differences with those developed by annealing in our runs.

It might be expected that, in a strongly strained rock submitted to a prolonged annealing, the syn- and post-tectonic recrystallizations would almost completely obliterate any large deformed grain as is the case with metals. An equant and equigranular mosaic texture would result. In fact we regard many crustal peridotites in deep seated terrains (for example, North Carolina and Ivrea zone peridotites) as natural examples of this process. It has also been observed in basalt xenoliths (equigranular texture, Mercier, 1972) and in garnet peridotites from kimberlites, where small unstrained and elongated crystals have grown inside the large strained ones (Boullier and Nicolas, 1973).

Kinematic analysis.—Bearing in mind the restrictions developed above (p. 865), the experiments confirm the validity of the proposed method of kinematic analysis of a plastically deformed peridotite massif (Nicolas, Bouchez, and Boudier, 1972) on the following points:

1. In a deformed crystal, it has been shown that the angle between the direction of maximum elongation and the glide axis (usually Z) resulted from simple shear by translation gliding inside the crystal (fig. 3). This angle indicates the direction of shearing and is related to the shear angle (fig. 5). This conclusion tends to support the statistical method, based on this principle, which is presented in our paper.

2. In experiments the grain size decreases with progressive strain (fig. 7A). This relation was asserted in the paper, and consequently maps of the shear intensity in the Lanzo massif were drawn.

CONCLUSIONS

From the experimental deformation of a synthetic dunite in dry environment (PT range: 13 to 15 kb; 1200° to 1300°C) with increasing strain from 0 to 58 percent (strain rates; 10^{-4} and 10^{-5}/sec), the following conclusions are drawn:

1. Starting from a random assemblage, with increasing strain a strong fabric is developed in the original olivine assemblage. [010] = X tends toward σ_1; [100] = Z and [001] = Y tend to lie in the flattening plane normal to σ_1.

2. From 0 percent to around 30 percent strain, the mechanism developing the fabric operates by rotation of the initially anisometric grains with subsidiary gliding and kinking; between 30 and 40 percent intracrystalline gliding in olivine is dominant (principal glide system [100] (010)). As a result, the grains are increasingly elongated and finally dismembered into smaller grains. They display many kink bands, the boundaries of which are normal to the flattening plane. This is due to bending during the flowage as predicted (Nicolas and others, 1971). In the glide process, deformation is not homogeneous and seems to concentrate in the regions of crystal boundaries. With over 40 percent strain, the syntectonic recrystallization becomes significant; it takes place mainly at the grain boundaries and might be induced by the high deformational energy stored in these domains. Plastic flow in quartzites experimentally produced by Tullis, Christie, and Griggs (1973) compares remarkably with these results. At 58 percent strain, after 10 hrs of stress-annealing at 1300°, the recrystallized grains grow sufficiently to form a mosaic structure; their total volume compares with that of the larger strained and elongated crystals deformed by gliding. In this discussion, we do not make a clear distinction between syntectonic and post-tectonic recrystallization (annealing); this is intentional. Our experiments suggest that in olivine the syntectonic recrystallization is not driven by the stress (Avé Lallemant and Carter, 1970) but by the strain through the stored strain energy as during primary annealing (Green, Griggs, and Christie, 1970).

3. Keeping in mind the restrictions presented (p. 865), the experimentally developed structures and fabrics compare very well with those of Alpine-type peridotites and many xenoliths (about 50 percent of the non-cumulates xenoliths from Western Europe and Hawaii). Both kinds of crystals representative of each mechanism have been described: the large strained elongated or dismembered crystals of olivine and enstatite deformed by gliding and the smaller polygonal grains due to syntectonic and post-tectonic recrystallization (Nicolas and others, 1971). In natural occurrences, the grain size is 5 to 10 times larger. Relying on the ratio of large strained crystal to small undeformed ones, the relative importance of gliding and syntectonic recrystallization is in favor of the first process except in intensely deformed peridotites (shear angle probably about 80°); in fact both processes can be closely connected, the crystals deformed by gliding readily recrystallizing, and the recrystallized crystals in turn gliding, as can be observed experimentally. Post-tectonic recrystallization (annealing) is variable; almost none for massifs deformed at lower temperature, important for massifs deformed around 1200° (Nicolas, Bouchez, and Boudier, 1972). It is suggested from the study of some xenoliths and crustal peridotites that annealing can almost completely obliterate the plastic deformation structure, leading to a coarse grained mosaic assemblage (Mercier, 1972).

4. The method of kinematic analysis of deformations in Alpine-type peridotites (Nicolas, Bouchez, and Boudier, 1972) is supported by experimental results that particularly confirm the following points: the grain size reduction can be correlated with the strain; the strain analysis of crystals deformed by gliding demonstrates the postulated relationship between the shear angle and the angle between the crystal elongation and the glide axis. The latter point, statistically considered, indicates that in many natural occurrences the deformation operates mainly by simple shear and subsidiarily by pure shear. The plane of shearing and the foliation make an angle α, which is related to the shear angle θ through the curve in figure 6.

5. The plastic flow structures and fabrics with dominant gliding are widespread. In high temperature intrusions, like the western Mediterranean lherzolites, they can be correlated with the intrusion movement (Nicolas, Bouchez, and Boudier, 1972; Nicolas and Jackson, 1972). In harzburgites connected with the ophiolite suite we consider them as representative of flow in the shallower oceanic mantle adjacent to the ridges and responsible for its seismic anisotropy (see below). In this case the post-tectonic recrystallization (annealing) is usually weak. The common occurrence of those structures and fabrics in xenoliths from the mantle underlying both continental and oceanic crusts (Mercier, 1972; Boullier and Nicolas, 1973) demonstrates the importance of this mechanism of flow in the areas of the mantle where the basalts and kimberlites generate. In those xenoliths the annealing is usually intense.

6. Since its discovery (Hess, 1964), the seismic anisotropy of the shallow oceanic mantle has been given many contradictory explanations, Lappin's (1971) being the most recent (for review, see Avé Lallement, and Carter, 1970). From field observations in Alpine-type peridotites and interpretation of the flow mechanism, we favor Francis's interpretation (1969). The field evidence indicates that the foliation approximates the plane of the flow and that it seems to be largely due to simple shear. In ophiolite complexes, the harzburgites with metamorphic and tectonic structure underlying the ultramafic and mafic cumulates (Nicolas and Jackson, 1972) have a well developed foliation. In some complexes where the subsequent deformations have not obliterated the original relationship, the foliation is parallel or close to the plane of magmatic settling (Red Mountain, Calif.; Vourinos, Moores, 1969; Newfoundland, Williams, 1971; Hatay-Bassit, Parot, personal commun.). Though this relation might not be general, it indicates that in a number of cases the foliation was horizontal, or nearly so, when the magmatic settling occurred. If the ophiolite suite is considered as representing a section of oceanic crust and mantle which originated at a ridge, the foliation in the mantle drifting from the ridge was consequently horizontal and the fabric connected to this plane is such that X tends to be vertical and Z and Y are in this plane. Regarding the foliation as due to shear, one would expect, like Francis, the direction of move-

ment, that is the glide direction Z in olivine and enstatite, to be normal or at a high angle to the ridge. Some ophiolite complexes (for example, eastern Papua, Davies, 1971; Newfoundland, Williams, 1971; Red Mountain, Calif.; Canyon Mountain, Oreg.) show evidence of plastic deformation in the lower levels of the cumulus sequence with development of a foliation that is traced down into the underlying harzburgites. This leads to the conclusion that the plastic flow responsible for the seismic anisotropy of the mantle was still active after the time when the foliation in the harzburgite mantle had reached the horizontal position under the ridge. This is not surprising considering that the temperature at the floor of the magmatic chamber was well over 1000° in order to precipitate ultramafic cumulates. In this respect, our conclusions differ from Francis's who proposed that the anisotropy was produced only during the ascent of convention currents.

ACKNOWLEDGMENTS

We are particularly grateful to E. D. Jackson, S. H. Kirby, and C. B. Raleigh for their help and guidance in the experimental work, to N. L. Carter, J. Goguel, and C. B. Raleigh for reviewing the manuscript. It was made possible with financial support from the U.S. Geological Survey and the French Délégation Générale pour la Recherche Scientifique et Technique.

APPENDIX

Calculation of the relation of the shear angle θ to the angle α between the direction of maximum elongation of an ellipse and the glide direction.*

This problem has a more general expression which can be stated as follows: starting with a segment d originating in O, the extremity A which is defined by x ($-\infty < x < +\infty$), what is the value of x corresponding to the maximum for the ratio D/d, D (OB) being the transformation of d by simple shear of the angle θ (fig. 9)?

Our particular problem can be related to the general one as illustrated by figure 10 where the long axis of the ellipse B'B is the transformation of one diameter A'A of the initial circle.

We have:

$$\frac{B'B}{A'A} = \frac{D}{d}$$

From figure 9 it can be demonstrated that:

$$d^2 = a^2 + x^2$$
$$D^2 = (a + b)^2 + x^2$$
$$b = x \tan\theta$$

We may decide that $a = 1$

$$\frac{D^2}{d^2} = \frac{(1 + x \tan\theta)^2 + x^2}{1 + x^2} = \frac{x^2 \tan^2\theta + x^2 + 2x \tan\theta + 1}{1 + x^2}$$

The maximum of D^2/d^2 and consequently of D/d is calculated for

$$\frac{d \dfrac{D^2}{d^2}}{dx} = 0$$

* By A. Etchecopar, Laboratoire de Géologie Structurale, Nantes, France.

$$\frac{d\ \frac{D^2}{d^2}}{dx} = 2 \tan\theta \frac{(1 - x^2 + x \tan\theta)}{(1 + x^2)^2} = 0$$

$(1 + x^2)^2$ is always positive and can be ignored. If $\tan\theta = 0$ the solution is indeterminate. For other values:

$$x = \frac{\tan\theta \pm \sqrt{\tan^2\theta + 4}}{2}$$

A second order derivation shows that the maximum considered is:

$$x = \frac{\tan\theta + \sqrt{\tan^2\theta + 4}}{2}$$

From figure 9, we have:

$$\cot\alpha = \frac{a + b}{x} = \frac{1 + x \tan\theta}{x}$$

$$\cot\alpha = \frac{2}{\tan\theta + \sqrt{\tan^2\theta + 4}} + \tan\theta$$

Using $\cot\alpha = \frac{1 - \tan^2\alpha}{2 \tan\alpha}$, this can be simplified to:

$$\cot 2\alpha = \frac{1}{2} \tan\theta$$

References

Avé Lallemant, H. G., 1967, Structural and petrofabric analysis of an "Alpine-type" peridotite: the lherzolite of the French Pyrenées: Leidse Geol. Meded., v. 42, p. 1-57.

Avé Lallemant, H. G., and Carter N. L., 1970, Syntectonic recrystallization of olivine and modes of flow in the upper mantle: Geol. Soc. America Bull., v. 81, p. 2203-2220.

Boullier, A. M., and Nicolas, A., 1973, Fabric analysis of the ultrabasic nodules from Thaba Putsoa and Mothae, *in* Kimberlites of the Northern Lesotho province: Cape and Transvaal Printers Ltd (1973).

Brothers, R. N., and Rodgers, K. A., 1969, Petrofabric studies of ultramafic nodules from Auckland, New Zealand: Jour. Geology, v. 77, p. 452-465.

Carter, N. L., and Avé Lallemant, H. G., 1970, High temperature flow of dunite and peridotite: Geol. Soc. America Bull., v. 81, p. 2181-2202.

Carter, N. L., Baker, D. W., and George, R. P., 1972, Seismic anisotropy, flow, and constitution of the upper mantle, *in* Flow and fracture of rocks (The Griggs Volume): Washington, D.C., Am. Geophys. Union.

Collée, A. L. G., 1963, A fabric study of lherzolites with special reference to ultrabasic nodular inclusions in the lavas of Auvergne (France): Leidse Geol. Meded., v. 28, p. 1-102.

Davies, H. L., 1971, Gabbro-basalt complex in Eastern Papua: an overthrust plate of oceanic mantle and crust: Australia Bur. Mineral Resources Bull., v. 128, 48 p.

Etienne, F., 1971, La lherzolite rubanée de Baldissero-Canavese: Univ. Nancy, thèse 3ème cycle, 150 p.

Francis, T. J. G., 1969, Generation of seismic anisotropy in the upper mantle along the mid-oceanic ridges: Nature, v. 221, p. 162.

Green, H. W., Griggs, D. T., and Christie, J. M., 1970, Syntectonic recrystallization and annealing of quartz aggregates, *in* Paulitsch, V. P. ed., Experimental and Natural Rock Deformation: Berlin/Heidelberg. Springer-Verlag, p. 272-335.

Griggs, D. T., 1967, Hydrolytic weakening of quartz and other silicates: Royal Astron. Soc. Geophys. Jour., v. 14, p. 19.

Hess, H. H., 1964, Seismic anisotropy of the uppermost mantle under the oceans: Nature, v. 203, p. 629.

Kumazawa, M., Helmstaedt, H., and Masaki K., 1971, Elastic properties of eclogite xenoliths from diatremes of the East Colorado Plateau and their implication to the upper-mantle structure: Jour. Geophys Research, v. 76, p. 1231-1247.

Lappin, M. A., 1971, The petrofabric orientation of olivine and seismic anisotropy of the mantle: Jour Geology, v. 79, p. 730-740.

Mercier, J. C., 1972, Structures des péridotites en enclaves dans quelques basaltes d'Europe et d'Hawaï. Regard sur la constitution du mainteau supérieur: Nantes, thése 3éme cycle, 229 p.

Möckel, J. R., 1969, Structural petrology of the garnet-peridotite of Alpe Arami (Ticino, Switzerland): Leidse Geol. Meded., v. 42, p. 61-130.

Moores, E. M., 1969, Petrology and structure of the Vourinos ophiolitic complex of Northern Greece: Geol. Soc. America Spec. Paper 118, 74 p.

Nicolas, A., and Jackson, E. D., 1972, Répartition en deux provinces des péridotites des chaines alpines longeant la Méditerranée: implications géotectoniques: Suisse Min. Pet. Bull., v. 52, p. 479-495.

Nicolas, A., Bouchez, J. L., and Boudier, F., 1972, Interprétation cinématique des déformations plastiques dans le massif de lherzolite de Lanzo (Alpes piémontaises). Comparaisons avec d'autres massifs: Tectonophysics, v. 14, p. 143-171.

Nicolas, A., Bouchez, J. L., Boudier, F., and Mercier, J. C., 1971, Textures, structures and fabrics due to solid state flow in some European lherzolites: Tectonophysics, v. 12, p. 55-86.

Raleigh, C. B., 1965, Structure and petrology of an Alpine peridotite on Cypress Island, Washington, U.S.A.: Contr. Mineralogy Petrology, v. 11, p. 719.

———— 1968, Mechanisms of plastic deformation of olivine: Jour. Geophys. Research., v. 73, p. 5396-5408.

Spry, A., 1969, Metamorphic textures: Oxford, Pergamon Press, 350 p.

Thayer, T. P., 1960, Some critical differences between Alpine-type and stratiform peridotite-gabbro complexes: Internat. Geol. Cong., 21st, Copenhagen 1960, Repts., Sess. 13, p. 247-259.

Tullis, J., Christie, J. M., and Griggs, D. T., 1973, Micro-structures and preferred orientations of experimentally deformed quartzite: Geol. Soc. America Bull., v. 84, p. 297-314.

Williams, H. W., 1971, Mafic-ultramafic complexes in Western Newfoundland Appalachians and the evidence for their transportation: a review and interim report: Geol. Assoc. Canada Proc., v. 24, p. 9-25.

Yoshino, G., 1964, Ultrabasic mass in the Higashiakaishi-yama district, Shikoku, Southwest Japan: Hiroshima Uni. Jour. Sci., ser. C, v. 4, p. 333-364.